Thin Film Growth Using Hetero Embryo: Demonstration on Pyrochlore Phase

A Pillonnet,*,† V. Le Bihan,† B. Masenelli,‡ G. Ledoux,† O. Marty,§ P. Mélinon,‡ and C. Dujardin†

Laboratoire de Physico-Chimie des Matériaux Luminescents, CNRS UMR 5620, Université de Lyon, Université Lyon 1, F-69622 Villeurbanne Cedex, France, Laboratoire PMCN, CNRS UMR 5586, Université Lyon 1, F-69622 Villeurbanne Cedex, France, and Institut des Nanotechnologies de Lyon (INL), CNRS UMR 5270, Université Claude Bernard Lyon, 43 bd du 11 novembre 1918, F-69622 Villeurbanne, France

ABSTRACT The paper reports the possible use of nanoparticles embedded in amorphous host as hetero embryos in order to grow complex crystalline phases as thin film. Demonstration is performed in the prototypical case of pyrochlore phase $Gd_2Ti_2O_7$ grown from Gd_2O_3 nanoparticles embedded in TiO_2 matrix at low temperature. As embryos, two kinds of nanoparticles are compared: clusters deposited by low energy cluster beam deposition (LECBD) and nanostructured films elaborated by sol-gel process. The growth has been analyzed by X-ray diffraction and transmission electron microscopy. Furthermore, the nanoparticles have been doped with Eu^{3+} luminescence probes in order to follow the nucleation mechanisms at the atomic scale. It is shown that the size, shape, and composition of hetero embryos and as well their interfaces are of paramount importance to enhance the formation of complex materials, such as pyrochlore. By this mean, the first step in classical nucleation science, controlling the height of the energetic barrier, is skipped and the synthesis conditions can be eased.

KEYWORDS: nanoparticles • pyrochlore $Gd_2Ti_2O_7$; interdiffusion • clusters • sol−gel

1. INTRODUCTION

The determination of the phase equilibrium data provides essential thermochemical guidance for advanced ceramic materials science. For this purpose, the ingredients to be monitored are the chemical composition, the temperature, the pressure, and the atmosphere. Unfortunately, the synthesis of complex oxides often requires severe conditions, as high temperature and pressure, which hinder their use in advanced microelectronic devices, nanotechnology applications and surface engineering. In the classical nucleation science, the crystal growth needs two steps: the formation of a stable embryo and the accretion around the embryo. But if there is no embryo or if no catalyst is known (homo nucleation), a hetero nucleation might be envisaged. In this case, the crystal nucleation is obtained by mixing embryos with different compositions. In fact, a detailed molecular model shows that initiation of stable crystals proceeds via a multitude of possible paths involving all types of nonequilibrium configurations that contribute to the kinetic barrier. The reduction of the thermodynamical cost of the first step would be a considerable breakthrough in crystal engineering, especially if we can discard the nonequilibrium configurations and thus directly control the nucleation rate. This can be contemplated by the use of nanoparticles as embryos. Because of the specifically high surface/volume ratio, it is well-known that nanomaterials have a higher chemical reactivity than their bulk analogues, and that their thermodynamical stability is highly modified. It allows then to bypass the standard phase diagram routes (1–4). Another route to obtain crystallites phases is the chemical sol-gel synthesis from organic precursor solution (5). In the literature, the interdiffusion between two different oxides has been often observed and used for powders (6, 7) or ceramics (8) synthesis by solid-state reaction. This effect in nanocrystalline insulators is more complex than in nanocrystalline metals due to the potential multiple phases and defect species (9). The diffusion into film has been studied in particular to control the interface quality (10) or to generate interface nanolayers (11), but this process is not used much for complex oxide elaboration. For instance zirconate titanate (PZT) thin films have been elaborated by diffusion into $PbZrO_3$ and $PbTiO_3$ alternate layers (12).

In this paper, we report the formation of thin films of $Gd_2Ti_2O_7$ pyrochlore by the embedding in an amorphous matrix (Ti_nO_m) of well-crystallized nanoparticles (Gd_2O_3) whose composition, shape, and size are known by previous studies (13–15). The isometric pyrochlore structure, with general formula of $A_2B_2O_7$, have a remarkable range of chemical, physical and electronic properties with a significant number of technological applications, as catalyst, matrix for nuclear waste, oxygen conductors in fuel cells (4). Its choice is further motivated by its lattice geometry leading to a highly frustrated antiferromagnet, where apart from the classical Heisenberg exchange, the spins interact via dipole−

* Corresponding author. E-mail: annep@pcml.univ-lyon1.fr.
Received for review March 10, 2010 and accepted April 30, 2010
† Laboratoire de Physico-Chimie des Matériaux Luminescents, CNRS UMR 5620, Université de Lyon.
‡ Laboratoire PMCN, CNRS UMR 5586, Université Lyon 1.
§ Institut des Nanotechnologies de Lyon (INL), CNRS UMR 5270, Université Claude Bernard Lyon.
DOI: 10.1021/am100203f

dipole forces (16, 17). Not much is known about the frustration effect in quasi-2D antiferromagnets. The magnetic frustration is expected to be greatly enhanced as one at least of the sample dimensions is reduced. Consequently, a great deal of effort is currently devoted to the synthesis of pyrochlore thin films. However, the scarce studies from the literature show that drastic conditions, such as high temperature, are needed to achieve thin films with moderate quality. In the present study, we show that pyrochlore thin films can be formed at a temperature lower than that of classical methods, which is the signature of the nucleation barrier dropping. This method can be extended to other materials and opens the way to the synthesis of quasi-2D advanced oxide compounds. The pyrochlore formation is studied at the atomic scale through the modification of the $^5D_0 \rightarrow {}^7F_J$ fluorescence lines of the Eu^{3+} ions. These ions are substituted to Gd^{3+} cations. The luminescence of the Eu^{3+} ion is strongly modified by the Stark effect induced by the lattice field and consequently probes the structure of the lattice formed by the surrounding atoms (18). Additional structural informations are given by X-ray diffraction (XRD) and transmission electron microscopy (TEM).

2. MATERIALS AND METHODS

The pyrochlore phases are mainly elaborated as polycrystallized powders using solid state reaction. The mixing of $Gd_2O_3 + 2TiO_2$ thermally treated at 1200°C allows the pyrochlore phase generation after the phase transition from Gd_2TiO_5 phase to $Gd_2Ti_2O_7$ (6). If the stoichiometry is not respected, only the Gd_2TiO_5 phase is obtained. The chemical sol−gel process using different chloride precursors in SiO_2 host allows decreasing the crystallization temperature at 1000°C (19). Lower temperature (780°C) can be obtained by mechanical milling synthesis (7). This process takes advantage of the perturbation of surface-bonded species by pressure to enhance thermodynamic and kinetic reactions between solids (20). Pyrochlore as film form has been elaborated only by classical sol−gel process (21). Nevertheless, a thermal treatment at 800°C induces a single diffraction line from the pyrochlore phase, but surprisingly the other ones are not present, revealing a moderate quality of the samples.

We propose here to use Gd_2O_3 nanoparticles embedded in TiO_2 host as hetero embryos to grow $Gd_2Ti_2O_7$ pyrochlore phase as thin film form with lower temperature treatment. We have tested Gd_2O_3 nanoparticles prepared by two different routes: low energy cluster beam deposition (LECBD) under high vacuum (13) and soft chemistry route based on sol−gel process (15).

The elaboration of nanoparticules through LECBD technique is detailed in references (13, 14, 22). Briefly, a target pellet made of Eu:Gd_2O_3 sintered powder, with Eu/Gd atomic ratio of 0.1, is hit by a pulsed YAG laser in a high vacuum chamber. A plasma is created and quenched by a synchronized helium burst (3 bars) starting the clusters nucleation. The plasma then undergoes a supersonic expansion through a nozzle. This adiabatic expansion freezes the nucleation of the clusters at an approximate rate of 1×10^{10} K s^{-1}. The clusters synthesis is far from the thermodynamic equilibrium conditions. The preformed clusters are then deposited at a pressure of 1×10^{-6} mbars on a substrate with sufficiently low kinetic energy (~0.5 eV per atom) to save their structure. The steady deposition rate controlled in situ by quartz balance is 0.17±0.04 Å/s. According to TEM study, the size of Eu:Gd_2O_3 clusters is 3±1 nm and their structure is cubic (13, 14).

The elaboration of Eu:Gd_2O_3 nanostructured layers by the sol-gel dip-coating process has been described in details elsewhere (15). In short, a Gd_2O_3 solution is elaborated by dilution of stabilized $Gd(CH_3COCHCOCH_3)_3$ powders (REacton) in ethanol under stirring at 90°C. Europium(III) nitrate pentahydrate (Aldrich) is added to obtain a Eu 10% mol-doped precursor solution. For film fabrication, silica substrates are then immersed in the solution and withdrawn from the bath at a rate of 40 mm/min. The layers obtained are first dried at 90°C for 5 min and subsequently heated at 600°C under a constant flow of dry oxygen for organic compounds elimination, film densification and crystallization. This process provides very small Eu:Gd_2O_3 crystallized nanoparticles of 3−5 nm diameter, comparable to LECBD clusters.

TiO_2 host films are elaborated by the same sol-gel dip-coating process (24). The TiO_2 solution is prepared using titanium isopropoxide ($Ti(O^iPr)_4$-Aldrich), iso-propanol (^iPrOH−Merck), acetic acid (AcOH-Prolabo) and diluted in methanol. The sol-gel layers thicknesses are deduced from the thicknesses of optical wave guiding multilayers measured by m-lines spectroscopy (23).

Both methods provide Eu:Gd_2O_3 nanocrystallites with similar size and structure. Nevertheless, films prepared under vacuum by LECBD, resulting from the deposition of preformed clusters, are foamlike (porosity around 70%), whereas films prepared by sol−gel are denser (porosity around 40%). The two kinds of Eu:Gd_2O_3 nanoparticles have been deposited as 30 nm thick film on a sol−gel TiO_2 bottom layer and have been covered with a second TiO_2 layer. The thickness of TiO_2 layers is evaluated at 30 nm. Because a 600 °C annealing is necessary to crystallize sol−gel Eu:Gd_2O_3 layers, all bottom TiO_2 layers have been annealed at this temperature and therefore crystallized in the anatase phase (24), even though preliminary studies have shown that interdiffusion is much easier through an amorphous substrate than a crystallized one. After covering, the two kinds of samples have been annealed step by step during 30 min up to 1000 °C using a Linkam TS1500 heating plate. In the following, the film that contains LECBD clusters is referred to as "LECBD sample", whereas the film prepared in full by the sol−gel process is labeled "sol−gel sample".

For each annealing step, the structure has been analyzed by XRD using a Siemens D500 diffractometer with Cu K_α radiation in grazing incidence configuration ($\theta = 0.5°$). After annealing at 1000 °C, the samples have been studied by TEM and high-resolution transmission microscopy (HRTEM) with a Topcom EM-002B microscope, working at 200 kV and using Kevex Sigma energy-dispersive X-ray equipment.

The europium photoluminescence (PL) spectra were recorded at room temperature by two experimental systems. The excitation at 290 nm has been obtained by a 450 W Xe lamp coupled to a Gemini 180 Jobin-Yvon monochromator with a band-pass of 2 nm. The excitation at 224 nm was realized with a photon 2000 He−Ag laser. The photoluminescence has been collected by an optical fiber and analyzed by a TRIAX 320 Jobin-Yvon monochromator and a Peltier cooled charge-coupled device detector ensuring a spectral resolution of 0.5 nm. The study of PL with temperature has been carried out using the heating plate in the PL set-up to preserve the excitation configuration in order to compare the PL intensities.

3. RESULTS AND DISCUSSION

The pyrochlore crystallization in different samples has been analyzed by XRD. The XRD patterns of both kinds of samples after annealing at 770 and 1000 °C are presented on Figure 1. Before 770 °C, the size of crystallites are too small to be detected by XRD. The diffraction lines of $Gd_2Ti_2O_7$ pyrochlore phases are clearly observed and ana-

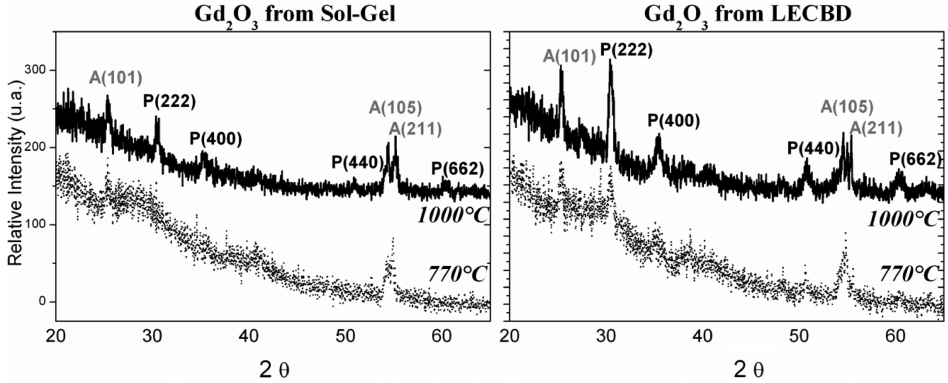

FIGURE 1. XRD pattern of pyrochlore thin films elaborated by interdiffusion of Eu: Gd_2O_3 nanoparticles (from sol−gel process and from LECBD) embedded in TiO_2 layers annealed at 700°C (in dotted) and at 1000°C (solid line). The line designations are P and A for pyrochlore $Gd_2Ti_2O_7$ and anatase TiO_2 phases, respectively.

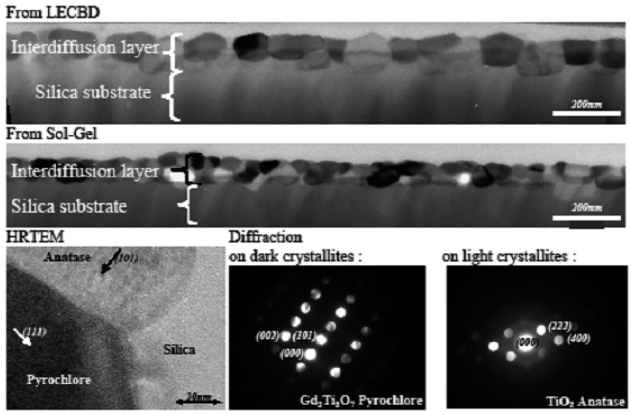

FIGURE 2. TEM bright-field images of pyrochlore thin films elaborated by interdiffusion of Eu: Gd_2O_3 nanoparticles (from sol−gel process and from LECBD) embedded in TiO_2 layers annealed at 1000°C. HRTEM images and diffraction patterns on dark and light crystallites allowing the phases identification are presented.

tase TiO_2 phase is also detected. This result is expected because in both samples the TiO_2 quantity is in excess stoichiometry and anatase is the phase observed after annealing up to 400 °C in sol−gel TiO_2 layer s (24). The analysis of XRD diffractograms by the Scherrer formula (25) shows that the estimated average size of crystallites is dependend on the *hkl* diffraction peak chosen for the calculations. Thus other sources of peak broadening like stresses must be considered. The XRD diffractograms of the films have been unregistered by optimizing the incidence angle in order to limit the substrate contribution. Nevertheless, the noise level of the patterns remains too high for Rietveld refinement.

TEM and HRTEM studies on the cross-section of both kinds of samples crystallized at 1000°C are presented in Figure 2. "LECBD sample" consists of a single layer of crystallites whose size is around 90 nm, whereas "sol−gel sample" appears in the form of multiple layers of smaller nanocrystallites whose size is around 50 nm. The results are roughly in agreement with XRD results, the observed crystallites sizes are larger than those estimated by the Scherrer formula, confirming the peak broadening by other sources. According to diffraction patterns, the dark particles are pyrochlore crystallites and the light gray ones are anatase TiO_2 crystallites. The HRTEM images confirm the phase designation. Although LECBD nanoparticles are used as embryos, the size of pyrochlore crystallites is larger, and thus LECBD nanoparticles appear to be better nucleation embryos than sol−gel layer ones. This result would be discussed after PL results.

As already mentioned, the Gd_2O_3 embryos are doped with Eu^{3+} activator ions in order to study crystallization at atomic scale during the nucleation process. It is known that Eu^{3+} ions substitute Gd^{3+} ions because Eu^{3+} and Gd^{3+} ions have similar ionic radii ($r_{Eu3+} = 0.98$ Å vs $r_{Gd3+} = 0.97$ Å (26)) and the same valence state. The Eu^{3+} emission corresponding to $^5D_0 \rightarrow {}^7F_J$ radiative transitions are reported in Figure 3. According to preliminary excitation studies, the PL spectra have been excited at 224 and 290 nm to favor Eu^{3+} emission in Gd_2O_3 and in $Gd_2Ti_2O_7$ phases, respectively (27). These excitation wavelengths corresponds to a direct excitation from valence band to conduction band in Gd_2O_3 (28) and $Gd_2Ti_2O_7$ (21). The positions of the main Eu^{3+} emission lines in cubic Gd_2O_3 phases (29), in $Gd_2Ti_2O_7$ phases (21, 30), and in TiO_2 phases (31) are reported in Figure 3 for comparison.

The PL spectra of "LECBD sample" annealed at 200°C present broad bands characteristic of disordered surrounding. This is due to the formation of hydroxyde shell when the clusters are in contact with air (13, 32). For the "sol−gel sample" annealed at the same temperature, the PL spectra present broad lines characteristic of very small size crystallites of cubic Gd_2O_3.

As the annealing temperature increases, two processes are competing: the growth of Eu:Gd_2O_3 nanoparticles due to clustering, and ions diffusion from nanoparticles to the TiO_2 surrounding media. As the annealing temperature increases up to 505 °C, the typical Eu^{3+} fluorescence lines in cubic Gd_2O_3 phase become narrower. "Sol−gel sample" (Figure 3 top left) exhibits a better crystallization than the "LECBD sample" (Figure 3 top right). The hydroxide shell around the Eu:Gd_2O_3 clusters probably slows down the aggregation, whereas in the sol−gel Eu:Gd_2O_3 film, crystallites are already in contact. Beyond 505 °C, the rise in temperature brings about an extinction of the cubic Eu:Gd_2O_3 lines in both samples. Desorption into TiO_2 media decreases the Eu:Gd_2O_3 nanoparticles size. The pyrochlore phase appears after an annealing at 655 °C for the "LECBD

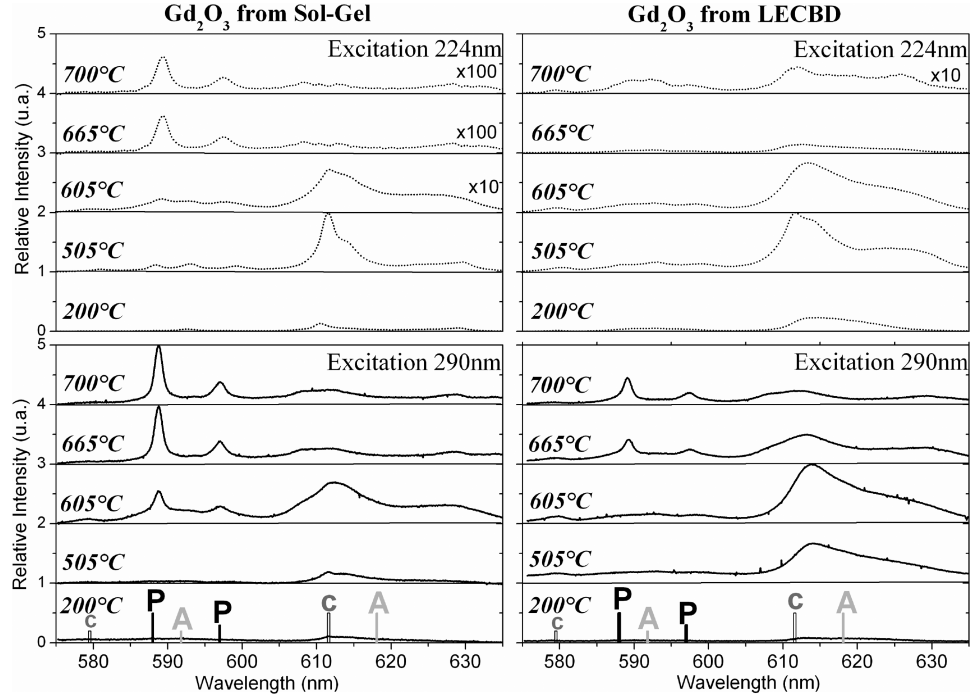

FIGURE 3. PL spectra (measured at room temperature) versus annealing temperature of thin films elaborated by interdiffusion of Eu:Gd_2O_3 nanoparticles (from sol−gel process and from LECBD) embedded on TiO_2 layers. The reference positions of the 2 main emission lines of Eu^{3+} in cubic Gd_2O_3 (c), pyrochlore (P) and anatase TiO_2 (A) phases are reported (top, excitation wavelength = 224 nm; bottom, excitation wavelength = 290 nm).

sample" and at 605 °C for the "sol−gel sample". Casually, we can notice that PL of Eu^{3+} ions is more accurate than XRD to probe the crystallization state at low temperature. However, the temperature difference between the two samples cannot be explained by hydroxide shell because it is completely eliminated by a heat treatment at 300 °C (13). We may then consider that the porosity difference is an important parameter.

The LECBD Eu:Gd_2O_3 layers are more porous than sol−gel ones. Their covering by dip-coating in TiO_2 sol probably causes the filling of a part of the pores. During treatment at low temperature, the ionic diffusion might be slowed down by air contained in pores. But the rise in annealing temperature induces a densification and removes pores filled with air. The high porosity becomes an advantage for pyrochlore nucleation because of higher surface contact between TiO_2 and Eu:Gd_2O_3 embryos. This explains the better crystallization state of the sample prepared by LECBD observed in XRD and TEM experience.

Note that no PL lines of Eu^{3+} ions in anatase TiO_2 phase has been detected in both samples when the thickness of deposited Eu:Gd_2O_3 layer is higher than 10 nm. In TiO_2 unlike in Gd_2O_3 or pyrochlore, Eu^{3+} ions occupy interstitial sites due to Ti^{4+} valence state and ionic radius difference ($r_{Ti4+} = 0.65$ Å vs $r_{Eu3+} = 0.98$ Å). Therefore the diffusion of Eu^{3+} in anatase is energetically less favorable. In addition if a Eu valence state change occurs, the PL of Eu^{2+} characterized by a broad band would be observed by scanning excitation wavelength of Xe lamp. This result means that hetero embryo nucleation needs enough Eu:Gd_2O_3 nanoparticles inside the TiO_2 matrix for the growth process, otherwise only TiO_2 matrix doping occurs.

Futhermore, we emphasize that even though TiO_2 is largely in excess around Eu:Gd_2O_3 nanoparticles, the growth process does not lead to amorphous or ill-defined compounds but strikingly to the complete $Gd_2Ti_2O_7$ phase and subsequently stops. The pyrochlore phase must thus be a global minimum of the energy diagram. This seems to be a critical feature in order to make our strategy efficient. Consequently, as soon as it is fulfilled, the hetero embryo-based nucleation seems a sound strategy to synthesize complex crystalline compounds at moderate growth conditions. In our study on $Gd_2Ti_2O_7$ phase, the growth temperature can be reduced by more than 30%, even though the inferior TiO_2 layer is crystallized. We can contemplate to reduce it further by depositing preformed nanoparticles on an amorphous substrate that will enhance the interdiffusion.

4. CONCLUSION

The embedding of Gd_2O_3 nanoparticles in Ti_2O host as hetero embryos allows growing complex crystalline phase as thin film form. During heat treatment, two processes predominate: the aggregation between nanoparticles and the diffusion of ions from nanoparticles into the surrounding media. These processes depend on the ions free energy which is more important for surface ions, promoting the use of nanoparticles (33). Consequently, the particles group together to minimize the energy or are destroyed in contact with surrounding by diffusion. The comparison between LECBD clusters and sol−gel film as nanoparticules shows that the crystallite growth depends on the chemical and structural properties of the nanoparticles layer and the effective surface in contact between the two embryos. As shown with the pyrochlore phase, this hetero embryo

nucleation technique is efficient to grow complex oxide at low temperature.

Acknowledgment. This work has been partially performed at the PLYRA (plateforme lyonnaise de recherche sur les agrégats) platform.

REFERENCES AND NOTES

(1) Joo, S. H.; Choi, S. J.; Oh, I.; Kwak, J.; Liu, Z.; Terasaki, O.; Ryoo, R. *Nature* **2001**, *412*, 169.
(2) Roduner, E. *Chem. Soc. Rev.* **2006**, *35*, 583.
(3) Schmidt, M.; Hippler, T.; Donges, J.; Kronmüller, W.; von Issendorff, B.; Haberland, H.; Labastie, P. *Phys. Rev. Lett.* **2001**, *87*, 203402.
(4) Lang, M.; Zhang, F.; Zhang, J.; Wang, J.; Schuster, B.; Trautmann, C.; Neumann, R.; Becker, U.; Ewing, R.C. *Nat. Mater.* **2009**, *8*, 793.
(5) Lange, F. F. *Science* **1996**, *273*, 903.
(6) Knop, O.; Brisse, F.; Castelliz, L.; Pyrochloes, V. *Can. J. Chem.* **1969**, *47*, 971.
(7) Fuentes, A. F.; Boulahya, K.; Maczka, M.; Hanuza, J.; Amador, U. *Solid State Sci.* **2005**, *7*, 343–353.
(8) Hreniak, D.; Zych, E.; Kepenski, L.; Strek, W. *J. Phys. Chem. Solids* **2003**, *64*, 111.
(9) Heitjans, P.; Indris, S. *J. Phys.: Condens. Matter* **2003**, *15*, R1257.
(10) Gallas, B.; Brunet-Bruneau, A.; Fisson, S.; Vuye, G.; Rivory, J. *J. Appl. Phys.* **2002**, *92*, 1922.
(11) Mistrik, J.; Lopusnik, R.; Visnovsky, S.; Keller, N.; Guyot, M.; Krishman, R. *J. Magn. Magn. Mater.* **2001**, *226*, 1820.
(12) Iijima, T.; He, G.; Funakubo, H. *J. Cryst. Growth* **2002**, *236*, 248.
(13) Masenelli, B.; Melinon, P.; Nicolas, D.; Bernstein, E.; Prevel, B.; Kapsa, J.; Boisron, O.; Perez, A.; Ledoux, G.; Mercier, B.; Dujardin, C.; Pellarin, M.; Broyer, M. *Eur. Phys. J. D* **2005**, *34*, 139.
(14) Nicolas, D.; Masenelli, B.; Mélinon, P.; Bernstein, E.; Dujardin, C.; Ledoux, G.; Esnouf, C. *J. Chem. Phys.* **2006**, *125*, 171104.
(15) Garcia-Murilo, A.; Le Luyer, C.; Dujardin, C.; Pedrini, C.; Mugnier, J. *Opt. Mater.* **2001**, *16*, 39.
(16) Greedan, J.E. *J. Alloys Compd.* **2006**, *408*, 444.
(17) Siddharthan, R.; Shastry, B. S.; Ramirez, A. P.; Hayashi, A.; Cava, R. ; Rosenkranz, S. *Phys. Rev. Lett.* **1999**, *83*, 1854 Ising.
(18) Cormier, G.; Capobianco, J. A.; Morrison, C. A.; Monteil, A. *Phys. Rev. B: Condens. Matter Mater. Phys.* **1993**, *48*, 16290.
(19) Lin, K. M.; Lin, C. C.; Li, Y. Y. *J. Lumin.* **2004**, *278*, 133.
(20) Gutman, E. *Mechanochemistry of Materials*; Cambridge International Science Publishing: Cambridge, U.K., 1997.
(21) Pang, M. L.; Lin, J.; Fu, J.; Cheng, Z. Y. *Mater. Res. Bull.* **2004**, *39*, 1607.
(22) Pellarin, M.; Ray, C.; Lerme, J.; Vialle, J. L.; Broyer, M.; Mélinon, P. *J. Chem. Phys.* **2000**, *112*, 8436.
(23) Ulrich, R.; Torge, R. *Appl. Opt.* **1973**, *12*, 2901.
(24) Bathat, A.; Bonazaoui, M.; Bathat, M.; Garapon, C.; Jacquier, B.; Mugnier, J. *J. Non-Cryst. Solid.* **1996**, *202*, 16.
(25) Patterson, A.L. *Phys. Rev.* **1939**, *56*, 978.
(26) Templeton, D. H.; Dauben, C. H. *J. Am. Chem. Soc.* **1954**, *76*, 5237.
(27) Le Bihan, V. Interactions de nano-objets luminescents (agrégats ou nano—films) avec leurs environnements:effets structuraux et diélectriques. PhD thesis, University Lyon 1, Villeurbanne, France, 2008.
(28) Prokofiev, A. V.; Shelykh, A. I.; Melekh, B. T. *J. Alloys Compd.* **1996**, *242*, 41.
(29) Garcia-Murilo, A.; Le Luyer, C.; Dujardin, C.; Martin, T.; Garapon, C.; Pedrini, C.; Mugnier, J. *Nucl. Instrum. Methods Phys. Res., Sect. A* **2002**, *486*, 181.
(30) McCauley, R. A.; Hummel, F. A. *J. Lumin.* **1973**, *6*, 105.
(31) Bouazaoui, M.; Bahtat, M.; Bahtat, A.; Mugnier, J. *J.Phys. IV* **1994**, *4*, 341.
(32) Wandelt, K.; Brundle, C. R. *Surf. Sci.* **1985**, *157*, 162.
(33) Sheng, H. W.; Lu et, K.; Ma, E. *Acta Mater.* **1998**, *46*, 5195.

AM100203F